

See discussions, stats, and author profiles for this publication at: <https://www.researchgate.net/publication/10985528>

# A NMR and Theoretical Study of the Aggregates between Alkylolithium and Chiral Lithium Amides: Control of the Topology through a Single Asymmetric Center

ARTICLE in JOURNAL OF THE AMERICAN CHEMICAL SOCIETY · JANUARY 2003

Impact Factor: 12.11 · DOI: 10.1021/ja016945d · Source: PubMed

---

CITATIONS

53

---

READS

22

11 AUTHORS, INCLUDING:



Catherine Fressigné

Université de Rouen

28 PUBLICATIONS 435 CITATIONS

SEE PROFILE



Anne Harrison-Marchand

Université de Rouen

49 PUBLICATIONS 625 CITATIONS

SEE PROFILE



Hassan Oulyadi

Université de Rouen

67 PUBLICATIONS 912 CITATIONS

SEE PROFILE

## A NMR and Theoretical Study of the Aggregates between Alkylolithium and Chiral Lithium Amides: Control of the Topology through a Single Asymmetric Center

Aline Corruble,<sup>†</sup> Daniel Davoust,<sup>‡</sup> Stéphanie Desjardins,<sup>‡</sup> Catherine Fressigné,<sup>†</sup> Claude Giessner-Prettre,<sup>\*,§</sup> Anne Harrison-Marchand,<sup>†</sup> Henri Houte,<sup>†</sup> Marie-Claire Lasne,<sup>⊥</sup> Jacques Maddaluno,<sup>\*,†</sup> Hassan Oulyadi,<sup>‡</sup> and Jean-Yves Valnot<sup>†</sup>

*Contribution from the Laboratoire des Fonctions Azotées & Oxygénées Complexes de l'IRCOF and Laboratoire de Chimie Organique et de Biologie Structurale, UMR 6014 CNRS, Université de Rouen, 76821 Mont St Aignan Cédex, France, Laboratoire de Chimie Théorique, UMR 7616 CNRS, Université P. & M. Curie, 4 place Jussieu, 75252 Paris Cédex 05, France, and Laboratoire de Chimie Moléculaire et Thioorganique, UMR 6507 CNRS, ISMRA, 6 Boulevard du Maréchal Juin, 14050 Caen Cédex, France*

Received August 27, 2001

**Abstract:** The complexes between methylolithium and chiral 3-aminopyrrolidine (3-AP) lithium amides bearing a second asymmetric center on their lateral amino group were studied using multinuclear (<sup>1</sup>H, <sup>6</sup>Li, <sup>13</sup>C, <sup>15</sup>N) low-temperature NMR spectroscopies in tetrahydrofuran-*d*<sub>6</sub>. The results indicate that lithium chelation forces the pyrrolidine ring of the 3-AP to adopt a norbornyl-like conformation and that robust 1:1 noncovalent complexes between methylolithium and 3-AP lithium amides form in the medium. A set of <sup>1</sup>H-<sup>1</sup>H and <sup>1</sup>H-<sup>6</sup>Li NMR cross-coupling correlations shows that the binding of methylolithium can take place along the “exo” or the “endo” face of this puckered structure, depending on the relative configuration of the lateral chiral group. This aggregation step renders the nitrogen of the 3-amino group chiral, the “exo” and “endo” topologies corresponding to the (*S*) and (*R*) configurations, respectively, of this atom. Density functional theory calculations show that the “exo” and “endo” arrangements are, for both diastereomers, almost isoenergetic even when solvent is taken into account. This result suggests that the formation of the mixed aggregates is under strict kinetic control. A relationship between the topology of these complexes and the sense of induction in the enantioselective alkylation of aromatic aldehydes by alkylolithiums is proposed.

### Introduction

Strict control of the stereogenic centers during the creation of carbon–carbon bonds remains a central concern in organic synthesis. The asymmetric condensation of an organometallic onto a carbonyl compound offers one of the most direct routes to achieve such a goal, and spectacular results have been reported with various reagents including organozinc (alone,<sup>1</sup> or catalyzed by various metals<sup>2</sup>), as well as organo-magnesium,<sup>3</sup> -chromium,<sup>4</sup> -titanium,<sup>5</sup> or -aluminum.<sup>6</sup> In most of these cases the metal is complexed by chiral polydentate ligands that behave not only as chemical activators but also as the source of asymmetry. Consequently, these ligands can be used catalytically, provided that the complexed organometallic is more

reactive than the uncomplexed reagent. By contrast, and because of their high intrinsic reactivity, organolithium species can only be engaged with difficulty in such processes.<sup>3c,7</sup> Nevertheless,

\* Corresponding author. E-mail: jmaddalu@crihan.fr.

<sup>†</sup> Laboratoire des Fonctions Azotées & Oxygénées Complexes, Université de Rouen.

<sup>‡</sup> Laboratoire de Chimie Organique et de Biologie Structurale, Université de Rouen.

<sup>§</sup> Laboratoire de Chimie Théorique, Université P. & M. Curie.

<sup>⊥</sup> Laboratoire de Chimie Moléculaire et Thioorganique, ISMRA de Caen.

(1) Reviews: (a) Noyori, R.; Suga, S.; Kawai, K.; Okada, S.; Kitamura, M. *Pure Appl. Chem.* **1988**, *60*, 1597–1606. (b) Soai, K.; Niwa, S. *Chem. Rev.* **1992**, *92*, 833–856. (c) Pu, L.; Yu, H. B. *Chem. Rev.* **2001**, *101*, 757–824.

- (2) Chromium: (a) Heaton, S. B.; Jones, G. B. *Tetrahedron Lett.* **1992**, *33*, 1693–1696. (b) Jones, G. B.; Heaton, S. B. *Tetrahedron: Asymmetry* **1993**, *4*, 261–272. Titanium: (c) Weber, B.; Seebach, D. *Tetrahedron* **1994**, *50*, 7473–7484. (d) Gennari, C.; Ceccarelli, S.; Piarulli, U.; Montalbetti, C. A. G. N.; Jackson, R. F. N. *J. Org. Chem.* **1998**, *63*, 5312–5313. (e) Pritchett, S.; Woodmansee, D. H.; Gantzel, P.; Walsh, P. J. *J. Am. Chem. Soc.* **1998**, *120*, 6423–6424. (f) Hwang, C. D.; Uang, B. J. *Tetrahedron: Asymmetry* **1998**, *9*, 3979–3984. (g) Shi, M.; Sui, W. S. *Tetrahedron: Asymmetry* **2000**, *11*, 835–841. (h) Prieto, O.; Ramon, O. J.; Yus, M. *Tetrahedron: Asymmetry* **2000**, *11*, 1629–1644. (i) Shen, X.; Guo, H.; Ding, K. *Tetrahedron: Asymmetry* **2000**, *11*, 4321–4327. (j) You, J. S.; Shao, M. Y.; Gau, H. M. *Organometallics* **2000**, *19*, 3368–3373.
- (3) (a) Battioni, J. P.; Chodkiewicz, W. *Bull. Soc. Chim. Fr.* **1972**, *5*, 2068–2069. (b) Meyers, A. I.; Ford, M. E. *Tetrahedron Lett.* **1974**, *14*, 1341–1344. (c) Mukaiyama, T.; Soai, K.; Sato, T.; Shimizu, H.; Suzuki, K. *J. Am. Chem. Soc.* **1979**, *101*, 1455–1460. (d) Tomioka, K.; Nakajima, M.; Koga, K. *Chem. Lett.* **1987**, 65–68. (e) Seebach, D.; Beck, A. K.; Imwinkelried, R.; Roggo, S.; Wonnacott, A. *Helv. Chim. Acta* **1987**, *70*, 954–974. (f) Weber, B.; Seebach, D. *Angew. Chem., Int. Ed. Engl.* **1992**, *31*, 4–86. (g) Nakajima, M.; Tomioka, K.; Koga, K. *Tetrahedron* **1993**, *49*, 9751–9758. (h) Weber, B.; Seebach, D. *Tetrahedron* **1994**, *50*, 6117–6128. (i) Saito, S.; Kano, T.; Hatanaka, K.; Yamamoto, H. *J. Org. Chem.* **1997**, *62*, 5651–5656.
- (4) (a) Chen, C.; Tagami, K.; Kishi, Y. *J. Org. Chem.* **1995**, *60*, 5386–5387. (b) Sujimoto, K.; Aoyagi, S.; Kibayashi, C. *J. Org. Chem.* **1997**, *62*, 2322–2323.
- (5) Reetz, M. T.; Kükenhöfner, T.; Weining, P. *Tetrahedron Lett.* **1986**, *27*, 5711–5714.

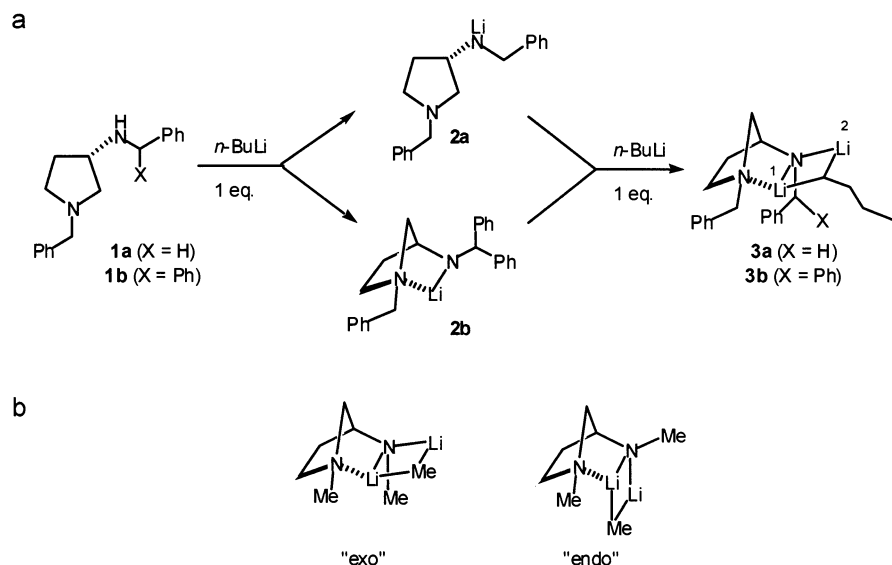


**Figure 1.** (a) Deprotonation of 3-aminopyrrolidines **1** and aggregation of corresponding lithium amides **2** with *n*-BuLi to form mixed complexes **3** (taken from ref 8d). (b) "endo" and "exo" modes for noncovalent aggregation (as defined in ref 13).

several recent studies, based on the pioneering work of Eleveld and Hogeveen,<sup>7c</sup> have clearly established that the noncovalent association between organolithium compounds and lithium amides can lead to aggregates sufficiently stable in solution to be used in the asymmetric nucleophilic alkylation of aldehydes.<sup>7f,g,8</sup> Various mixed dimers between alkylolithiums and lithium amides in a 1:1 ratio have been observed in solution,<sup>8a,b,d,g</sup> whereas three cases of 1:2 complexes<sup>9</sup> have been described, mainly in the solid state. Few theoretical studies have been dedicated to the mixed aggregation problem<sup>10</sup> and a study on the physicochemical forces responsible for this complexation have led to the conclusion that the electrostatic forces play a major role in this interaction.<sup>11</sup> Actually, the chemoselectivity of a system gathering two competitive nucleophilic entities such as an alkylolithium and a lithium amide can be difficult to predict, the formation of an  $\alpha$ -amino alcoholate having been shown experimentally (directly<sup>12</sup> and indirectly<sup>8c</sup>) as well as theoretically.<sup>10a</sup> Therefore, the ideal chiral amine to be used in such a

reaction requires structural elements allowing a high induction potential and a low nucleophilicity toward carbonyl compounds. Finally, an important practical requirement for the system versatility is the availability of both amine enantiomers.

Our previous work on the behavior of 3-aminopyrrolidines (3-AP) as chiral ligands has led to the conclusion that the conformation of their lithium amides in solution depends on the bulkiness of the lateral amine substituent.<sup>8d</sup> Thus, whereas 3-benzylaminopyrrolidine **2a** in tetrahydrofuran (THF) at low temperature yields an undetermined oligomeric mixture, 3-diphenylmethyl-aminopyrrolidine lithium amide **2b** undergoes, in the same conditions, a chelation of the lithium atom by the pyrrolidine nitrogen, leading to an aza-norbornyl structure (Figure 1a), as established on both spectroscopic<sup>8d</sup> and theoretical<sup>13</sup> grounds. In the presence of an excess of butyllithium, we have described the formation of 1:1 aggregates **3**, in which the norbornyl-like arrangement of the diamino moiety occurs whatever the lateral substituent (Figure 1a). At this stage, the butyllithium thus becomes "chiral" and, in the hypothesis that such an intermediate is responsible for the observed inductions, it explains in terms of "diastereoselectivity" the overall enantioselective process described in Scheme 1. These complexes have been tested in the asymmetric alkylation of aldehydes, and the highest enantiomeric excesses (ee's) were obtained with *o*-tolualdehyde.

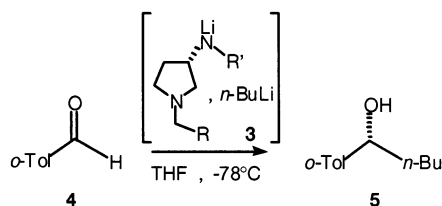
Our previous results have shown that the induction level is highly sensitive to the structure of the lateral chain, and that the sense of the induction can even be tuned through the introduction of a second asymmetric center on this same position.<sup>8e</sup> Hence, the selectivity of the alkylation is largely reversed when the  $\alpha$ -methylbenzyl appendage is switched from (*R*) to (*S*) (Table 1, entries 3 and 4).

To check the generality of this phenomenon and to try to correlate chemical results and structural data, we have extended our investigations to: (1) the induction potential of new 3-AP

- (6) (a) Chan, A. S. C.; Zhang, F. Y.; Yip, C. W. *J. Am. Chem. Soc.* **1997**, *119*, 4080–4081. (b) Pagenkopf, B. L.; Carreira, E. M. *Tetrahedron Lett.* **1998**, *39*, 9593–9596. (c) Lu, J. F.; You, J. S.; Gau, H. M. *Tetrahedron: Asymmetry* **2000**, *11*, 2531–2535.
- (7) (a) Nozaki, H.; Aratani, T.; Toraya, T. *Tetrahedron Lett.* **1968**, 4097–4098. (b) Mazaleyrat, J. P.; Cram, D. J. *J. Am. Chem. Soc.* **1981**, *103*, 4585–4586. (c) Eleveld, M. B.; Hogeveen, H. *Tetrahedron Lett.* **1984**, *25*, 5187–5190. (d) Mukaiyama, T.; Asami, M. *Top. Curr. Chem.* **1985**, *127*, 133–167. (e) Kanoh, S.; Muramoto, H.; Maeda, K.; Kawaguchi, N.; Motoi, M.; Suda, H. *Bull. Chem. Soc. Jpn.* **1988**, *61*, 2244–2246. (f) Schön, M.; Naef, R. *Tetrahedron: Asymmetry* **1999**, *10*, 169–176. (g) Arvidsson, P. I.; Hilmersson, G.; Davidsson, Ö. *Chem. Eur. J.* **1999**, *5*, 2348–2355.
- (8) (a) Hilmersson, G.; Davidsson, Ö. *J. Organomet. Chem.* **1995**, *489*, 175–179. (b) Hilmersson, G.; Davidsson, Ö. *J. Org. Chem.* **1995**, *60*, 7660–7669. (c) Corruble, A.; Valnot, J. Y.; Maddaluno, J.; Duhamel, P. *Tetrahedron: Asymmetry* **1997**, *8*, 1519–1523. (d) Corruble, A.; Valnot, J. Y.; Maddaluno, J.; Prigent, Y.; Davoust, D.; Duhamel, P. *J. Am. Chem. Soc.* **1997**, *119*, 10042–10048. (e) Corruble, A.; Valnot, J.-Y.; Maddaluno, J.; Duhamel, P. *J. Org. Chem.* **1998**, *63*, 8266–8275. (f) Arvidsson, P. I.; Davidsson, Ö.; Hilmersson, G. *Tetrahedron: Asymmetry* **1999**, *10*, 527–534. (g) Eriksson, J. E.; Arvidsson, P. I.; Davidsson, Ö. *Chem. Eur. J.* **1999**, *5*, 2356–2361.
- (9) (a) Williard, P. G.; Sun, C. *J. Am. Chem. Soc.* **1997**, *119*, 11693–11694. (b) Van Vliet, G. L. J.; Luitjes, H.; Schakel, M.; Klumpp, G. W. *Angew. Chem., Int. Ed. Engl.* **2000**, *39*, 1643–1645. (c) Hilmersson, G.; Malmros, B. *Chem. Eur. J.* **2001**, *7*, 337–341.
- (10) (a) Fressigné, C.; Maddaluno, J.; Marquez, A.; Giessner-Prettre, C. *J. Org. Chem.* **2000**, *65*, 8899–8907. (b) Haeflner, F.; Sun, C.; Williard, P. G. *J. Am. Chem. Soc.* **2000**, *122*, 12542–12546. (c) Hayes, J. M.; Greer, J. C.; Mair, F. S. *New J. Chem.* **2001**, 262–267.
- (11) Fressigné, C.; Maddaluno, J.; Giessner-Prettre, C. *J. Chem. Soc., Perkin Trans. 2* **1999**, 2197–2201.

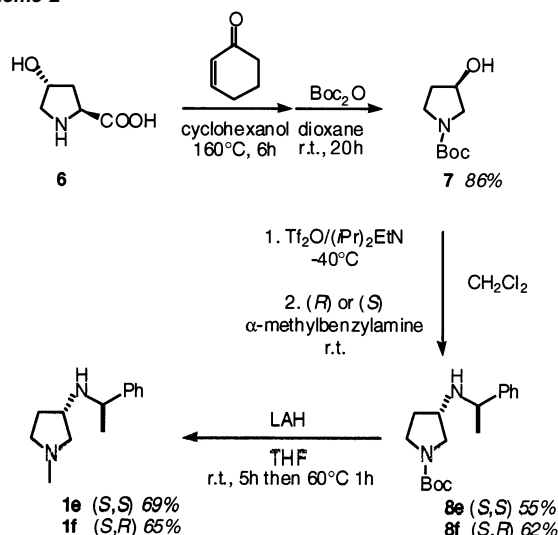
- (12) (a) Commins, D. L. *Synlett* **1992**, 615–625. (b) Juaristi, E.; Beck, A. K.; Hansen, J.; Matt, T.; Mukhopadhyay, T.; Simson, P.; Seebach, D. *Synthesis* **1993**, 1271–1289.
- (13) Fressigné, C.; Corruble, A.; Valnot, J.-Y.; Maddaluno, J.; Giessner-Prettre, C. *J. Organomet. Chem.* **1997**, *549*, 81–88.

Scheme 1

**Table 1.** Chiral Induction by Amides **2a,f** in the Enantioselective Alkylation of *o*-Tolualdehyde by Butyllithium (Scheme 1)

entry	amide	R	R'	Yd (%)	ee (%)	ref
1	<b>2a</b>	Ph	CH <sub>2</sub> Ph	57	49 ( <i>R</i> )	8e
2	<b>2b</b>	Ph	CHPh <sub>2</sub>	77	73 ( <i>R</i> )	8e
3	<b>2c</b>	$\beta$ -naphthyl	CHMePh ( <i>S</i> )	91	51 ( <i>S</i> )	8e
4	<b>2d</b>	$\beta$ -naphthyl	CHMePh ( <i>R</i> )	95	77 ( <i>R</i> )	8e
5	<b>2e</b>	H	CHMePh ( <i>S</i> )	66	74 ( <i>S</i> )	this work
6	<b>2f</b>	H	CHMePh ( <i>R</i> )	45	80 ( <i>R</i> )	this work

Scheme 2



lithium amides **2e,f**, prepared from amines **1e,f** (see Scheme 2), complexed with *n*-butyllithium; (2) the NMR study of amides **2c–f** as well as their complexes with methyllithium; (3) the density functional theory (DFT) study of amides **2e,f** and their complexes with methyllithium. The calculations were undertaken to compare the structures deduced from spectroscopy to those obtained from quantum chemistry, and to evaluate an eventual solvent effect on each complex conformation, taking into account three molecules of dimethyl ether, an appropriate model of THF. The importance of solvation on the aggregation of organolithiated species, particularly in the case of etheral media such as THF, is well established.<sup>14</sup> We present hereafter the results of this three-fold study and the structure of the reactive intermediates that have been deduced and try to relate it to the

strong influence of the lateral asymmetric center on the sense of the induction in this reaction.

## Results and Discussion

**Synthesis and Evaluation of New Diastereomeric 3-AP **2e** and **2f**.** The relatively modest influence of the substituent borne by the cyclic nitrogen of the 3-AP on the reaction of Scheme 1 has been previously shown.<sup>8e</sup> To clarify the NMR spectra and to simplify the multinuclear study, we synthesized 3-AP with a “minimal” alkyl chain on this position, namely, a methyl group. This was achieved through the decarboxylation of 4-(*R*)-hydroxy-L-proline **6**, following the efficient Houghton procedure (Scheme 2).<sup>15</sup> The intermediate 3-(*R*)-hydroxypyrrolidine thus obtained was not isolated but reacted directly with di-*tert*-butyl dicarbonate (Boc<sub>2</sub>O), leading to **7**. The second chiral center derived from the (*R*) or (*S*)  $\alpha$ -methylbenzylamine was then introduced through a nucleophilic substitution on the triflate, generated *in situ* from alcohol **7** and triflic anhydride [(CF<sub>3</sub>-SO<sub>2</sub>)<sub>2</sub>O] at low temperature. The reduction of the aminoamide **8** with lithium aluminum hydride (LAH) in THF at room temperature provided both (*S,R*) and (*S,S*) diastereomers of *N*-methyl-3-(*S*)-aminopyrrolidines **1e** and **1f**, respectively.<sup>8e</sup> The overall yields are approximatively 35% and the diastereomeric excesses (as determined by 500 MHz NMR) are about 95%.

These two new diamines were tested in the asymmetric alkylation reaction represented in Scheme 1, according to a procedure previously optimized.<sup>8c,e</sup> Experimentally, 1.5 equiv of 3-AP was diluted into THF at  $-20^{\circ}\text{C}$  and 1.6 equiv of BuLi followed by another 1.5 equiv of BuLi were added before cooling to  $-78^{\circ}\text{C}$  and final addition of 1 equiv of *o*-tolualdehyde. The enantiomeric excesses measured by chiral HPLC (on a Chiralcel OD column) on the 1-*o*-tolyl-1-pentanol **5** recovered after workup are reported in Table 1 (entries 5 and 6) together with those previously determined using the  $\beta$ -naphthyl analogues **1c,d** (Figure 2) following the same protocol.<sup>8e</sup> These results indicate that the reversal in the sense of induction, as observed when going from **2e** to **2f**, remains essentially controlled by the lateral asymmetric center but can be modulated to a significant extent by the substituent on the ring nitrogen, increasing the initial ee from 51 to 74% in the case of the (*3S,8S*) enantiomers (**2c** and **2e**). These data are also of practical importance because they suggest that both enantiomers of alcohol **5** can be obtained, from a single chiral pyrrolidinic scaffold, by simply inverting the lateral amino chain, which is in this case one of the cheapest chiral amines available in both enantiomeric forms.

**Multinuclear NMR Study of Complexes **3c–f** between Lithium Amides **2c–f** and Methyllithium.** Our previous work on this family of compounds focusing on aggregates **3a,b** between 3-AP lithium amides **2a** and **2b**, bearing one single asymmetric center on the pyrrolidine ring, and butyllithium<sup>8c–e</sup> revealed 1:1 complexes of the type **2** (Figure 1a). The folded pyrrolidine moiety and the butyllithium in **2** are noncovalently (but relatively strongly) side-bonded and the C–Li bond is oriented more or less parallel to one of the N–Li bonds. The <sup>6</sup>Li/<sup>1</sup>H heteronuclear Overhauser effect spectroscopy (HOESY) experiments also indicated that the butyl residue points toward the “exo” face of the aza-norbornyle structure (i.e., in the C<sup>2</sup>

(14) See for instance: (a) Seebach, D. *Angew. Chem., Int. Ed. Engl.* **1988**, *27*, 1624–1654. (b) Armstrong, D. R.; Mulvey, R. E.; Walker, G. T.; Barr, D.; Snaith, R.; Clegg, W.; Reed, D. *J. Chem. Soc., Dalton Trans.* **1988**, 617–628. (c) Kaufmann, E.; Gose, J.; Schleyer, P. v. R. *Organometallics* **1989**, *8*, 2577–2584. (d) Reich, H. J.; Kulicke, K. J. *J. Am. Chem. Soc.* **1996**, *118*, 273–274. (e) Henderson, K. W.; Dorigo, A. E.; Liu, Q.-Y.; Williard, P. G. *J. Am. Chem. Soc.* **1997**, *119*, 11855–11863. (f) Hilmersson, G.; Arvidsson, P. I.; Davidsson, Ö.; Håkansson, M. *Organometallics* **1997**, *16*, 3352–3362. (g) Arvidsson, P. I.; Davidsson, Ö. *Angew. Chem., Int. Ed. Engl.* **2000**, *39*, 1467–1470. (h) Sun, X.; Collum, D. B. *J. Am. Chem. Soc.* **2000**, *122*, 2459–2463. (i) Hilmersson, G. *Chem. Eur. J.* **2000**, *6*, 3069–3075. (j) Rutherford, J. L.; Collum, D. B. *J. Am. Chem. Soc.* **2001**, *123*, 199–202.

(15) Houghton, P. G.; Humphrey, G. R.; Kennedy, D. J.; Roberts, D. C.; Wright, S. H. B. *J. Chem. Soc., Perkin Trans. 1* **1993**, 1421–1424.



direction; Figure 1b). Actually, Li<sup>2</sup> showed clear through-space correlations with one bridging H<sup>2</sup> proton.<sup>8d</sup> The conformation of the 3-AP lithium amides alone and complexed as deduced from the NMR could be supported by ab initio theoretical calculations.<sup>13</sup>

We assumed that this type of complex could be responsible for the asymmetric inductions observed in the asymmetric alkylation of aldehydes (Table 1, entries 1 and 2), although this could not be established directly on the basis of spectroscopic evidence. A similar reaction, involving (BuLi)<sub>4</sub>, has been shown to be extremely rapid on the NMR timescale,<sup>16</sup> and the inductions observed tend to suggest that the mixed aggregates are more reactive than (BuLi)<sub>4</sub>. The influence of a second asymmetric center borne by the lateral amino group on the structure of these complexes had previously been observed but left unexplained. The strong effect of this parameter on the inductions obtained (Table 1, entries 3–6) prompted us to undertake a comparable multinuclear NMR study on these species. Determining the conformation of these complexes could be of major importance because it could help to get an insight into the docking of the aldehyde onto the complex and the fine details of its interaction with the alkyllithium during the condensation. Understanding the arrangement of the lateral chiral group required the unequivocal assignment of the 1.23-ppm doublet of the methyl group of the  $\alpha$ -methylbenzylamino appendage, and its clear separation from other confounding signals. The complex butyllithium multiplet in the same region

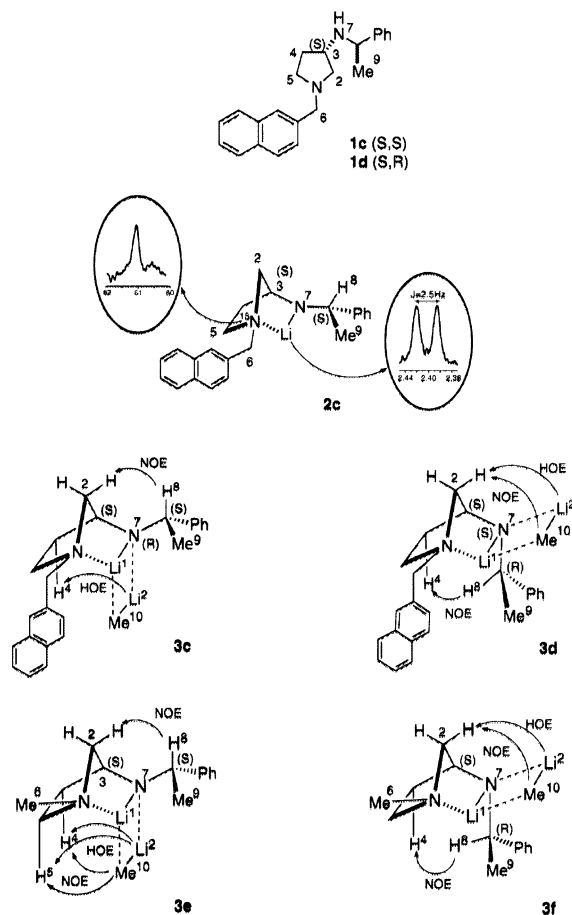


**Figure 2.** Structures of amines **1c**, **1d** and proposed conformations for lithium amide [<sup>6</sup>Li]-**2c** and mixed-aggregate [<sup>6</sup>Li]-**3c**, **3d**, **3e**, and **3f** in THF-d<sub>8</sub> solution at −78 °C.

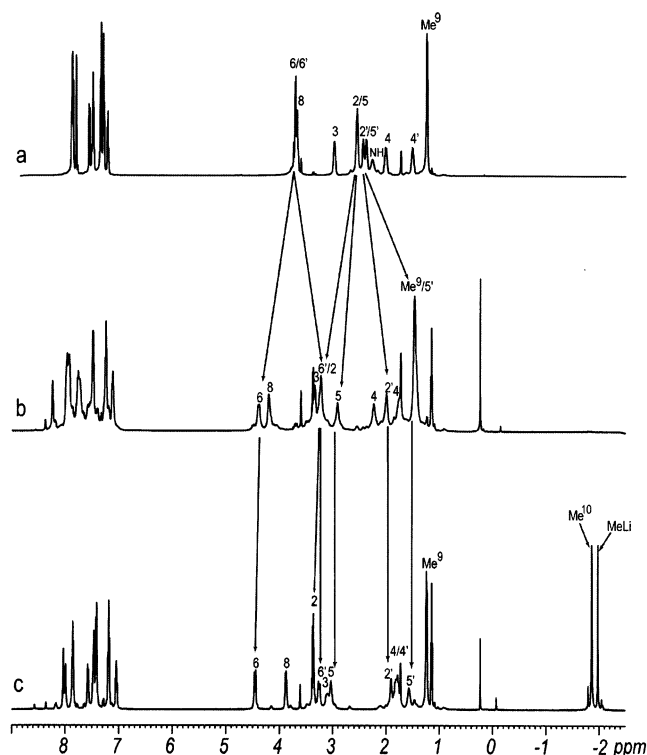


**Figure 3.** <sup>1</sup>H NMR spectra (THF-d<sub>8</sub>, −78 °C, 500 MHz) of amine **1c** (a), lithium amide [<sup>6</sup>Li]-**2c** (b), and mixed-aggregate [<sup>6</sup>Li]-**3c** (c).

necessitated the use of methyllithium which gives a sharp singlet well separated at −2.00 ppm. This swap was expected to be of limited consequence because previous experiments showed that methyllithium also adds with high enantioselection.<sup>8e</sup> The sensitivity of the complex structures to alkyllithium was also expected to be relatively limited, considering that their formation is probably under kinetic control (*vide infra*). This statement is supported by Williard's observation regarding the similarity of the mixed aggregates formed between butyl, *sec*-butyl or *tert*-butyllithium and *N*-isopropyl-*O*-methyl valinol lithium amide.<sup>9a</sup>

The salt-free <sup>6</sup>Li-methyllithium was prepared under ultradry argon from commercial <sup>6</sup>Li, amalgamated with 0.5% Na, and methyl chloride in diethyl ether at room temperature using a procedure adapted from Kamienski.<sup>17</sup> The methyllithium was dried down and redissolved in THF-d<sub>8</sub>. This solution could be kept in the freezer for only a few days, whereas the original ether solution is remarkably stable.

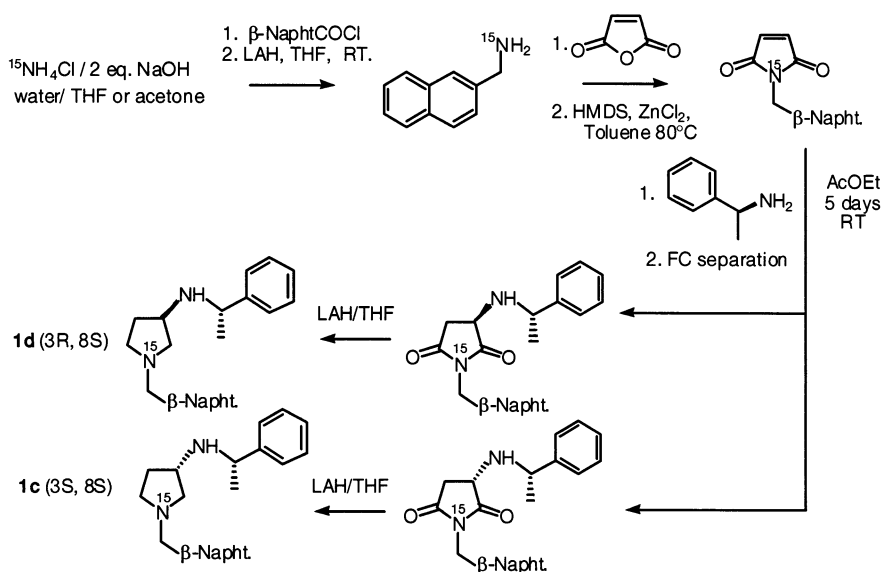
**(3*S*,8*S*)-*N*- $\beta$ -Naphthyl **2c/3c**.** The case of lithium amide **2c** and of its complex with methyllithium was investigated first. A  $\approx$ 0.3 M solution of amide in THF-d<sub>8</sub> was prepared in the NMR tube by rapid addition at −78 °C of one equiv of Me<sup>6</sup>Li on the amine **1c** solution (Figure 2). The <sup>1</sup>H NMR spectrum recorded at this temperature indicates a strong splitting of the signals of three proton groups, namely, H<sup>2</sup>, H<sup>5</sup>, and H<sup>6</sup> (Figure 3). This observation is identical to that previously made for amide **2b** and is associated with the folding of the pyrrolidine ring (Figure 1a). In addition, H<sup>8</sup> shifts from 3.67 ppm in the amine to 4.20 ppm in the amide.

The <sup>6</sup>Li spectrum displays a sharp singlet at 2.51 ppm, together with a smaller unidentified singlet (see Figure 1S of

(16) (a) McGarrity, J. F.; Ogle, C. A. *J. Am. Chem. Soc.* **1985**, *107*, 1805–1810. (b) McGarrity, J. F.; Ogle, C. A.; Brich, Z.; Loosli, H.-R. *J. Am. Chem. Soc.* **1985**, *107*, 1810–1815.

(17) Kamienski, C. W.; Esmay, D. L. *J. Org. Chem.* **1960**, *25*, 1807–1809.

Scheme 3



Supporting Information or  $^6\text{Li}$  projection in Figure 4). Therefore, this lithium amide seems to provide mainly one species, symmetrical if aggregated, as previously observed for the more cumbersome amide **2b**. It is, however, difficult to differentiate a dimeric (higher oligomers being unlikely because of the steric hindrances) from a monomeric structure without resorting to  $^{15}\text{N}$  labeling of the lateral amino group. Because the synthesis of chiral  $^{15}\text{N}$ - $\alpha$ -methylbenzylamine is not simple, we resorted to  $^{15}\text{N}$  labeling of the pyrrolidinic ring (prepared from commercially available  $^{15}\text{NH}_4\text{Cl}$ ; Scheme 3), expected to provide instead unequivocal evidence for the folding of the structure.

The  $^6\text{Li}$ ,  $^{15}\text{N}$ -labeled amide **2c** exhibits a  $^6\text{Li}$  spectrum in which the previous singlet appears as a doublet ( $J = 2.5$  Hz; Figure 2). This value is in excellent agreement with that calculated ( $-2.2$  Hz)<sup>18</sup> for a  $(\text{Me}_2\text{NLi}-\text{NMe}_3\cdot 2\text{H}_2\text{O})$  aggregate taken as a model for solvated **2c** and that was measured (2.7 Hz) by

Gawley et al.<sup>19</sup> on  $\alpha$ -aminoorganolithium compounds. Additionally, the  $^{15}\text{N}$  spectrum shows a large singlet at  $\delta = 61.1$  ppm (Figure 2), the coupling being too small to be resolved at 50 MHz (the  $^{15}\text{N}$  frequency on our spectrometer). The  $^6\text{Li}$  signal undergoes, as expected for the NMR one-bond isotopic effect,<sup>20</sup> a shift to higher field ( $\Delta\delta = 0.11$  ppm) upon going from  $^{14}\text{N}$  to  $^{15}\text{N}$ . The ring folding was further confirmed by two-dimensional NMR experiments. First, a  $^6\text{Li}/^1\text{H}$  HOESY experiment exhibited strong correlation cross-peaks between the lithium and protons  $\text{H}^6$ ,  $\text{H}^8$ , and  $\text{Me}^9$  (Figure 4). This experiment also gave indications on the arrangement of the chiral lateral group that is probably oriented as depicted in Figure 2. Finally, it is worth noting that if **2c** is monomeric, it should adopt a more-or-less planar topology, as established in a few cases,<sup>21</sup> such as complexed lithium bis(trimethylsilyl)amide ( $\text{LiHMDS}$ ), by X-ray crystallography, and confirmed by recent theoretical results.<sup>22</sup> We have not further investigated the structure of this intermediate because the species of primary interest is the methylolithium complex.

The addition of 1.4 equiv of methylolithium to **2c** led to the expected 1:1 complex **3c** (Figure 2). This arrangement was determined through a set of one- and two-dimensional NMR experiments. The  $^1\text{H}$  NMR spectrum (Figure 3c) is well resolved and the assignment of the signals was achieved by  $^1\text{H}/^1\text{H}$  correlation spectroscopy (COSY) and  $^1\text{H}/^{13}\text{C}$  heteronuclear multiple-quantum coherence (HMQC) (Figures 2S and 3S), as well as  $^1\text{H}/^1\text{H}$  nuclear Overhauser effect spectroscopy (NOESY) (Figure 5a) experiments. The chemical shifts are similar to those determined for **2c**, except for protons  $\text{H}^4$  (that merge in a multiplet at  $\approx 1.80$  ppm) and  $\text{H}^8$  (that moves back to a higher field at  $\approx 3.88$  ppm). This suggests that the folding of the pyrrolidine is conserved, as confirmed below by a double-labeling experiment. A singlet appears at negative shifts (at  $-1.86$  ppm) which was assigned to the complexed methylolithium  $\text{Me}^{10}$ , together with another singlet (at  $-1.97$  ppm), corresponding to the excess of methylolithium (probably tetrameric in THF)<sup>23</sup> introduced in the tube.

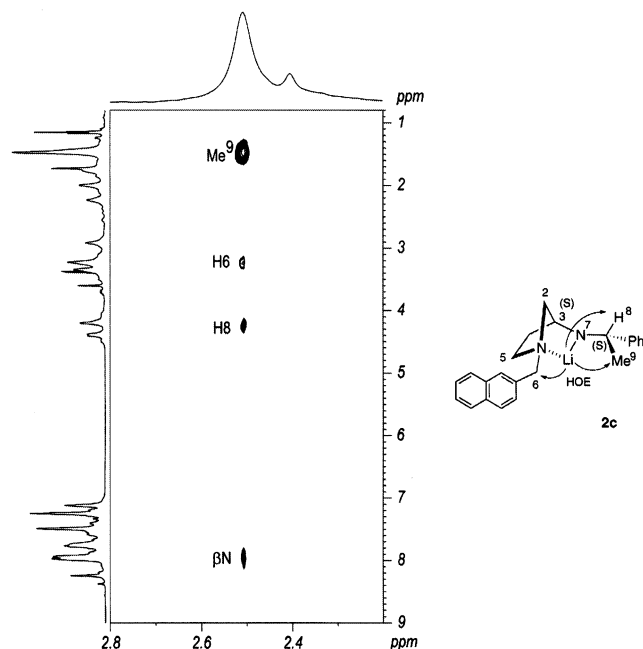


**Figure 4.** Two-dimensional  $^6\text{Li}/^1\text{H}$  HOESY contour plot ( $\tau_m = 1$  s) of lithium amide  $[\text{}^6\text{Li}]\text{-2c}$ .

(18) Parisel, O.; Fressigné, C.; Maddaluno, J.; Giessner-Prettre, C., submitted for publication.

(19) Low, E.; Gawley, R. E. *J. Am. Chem. Soc.* **2000**, *122*, 9562–9563.

(20) Günther, H. *J. Braz. Chem. Soc.* **1999**, *10*, 241–262.

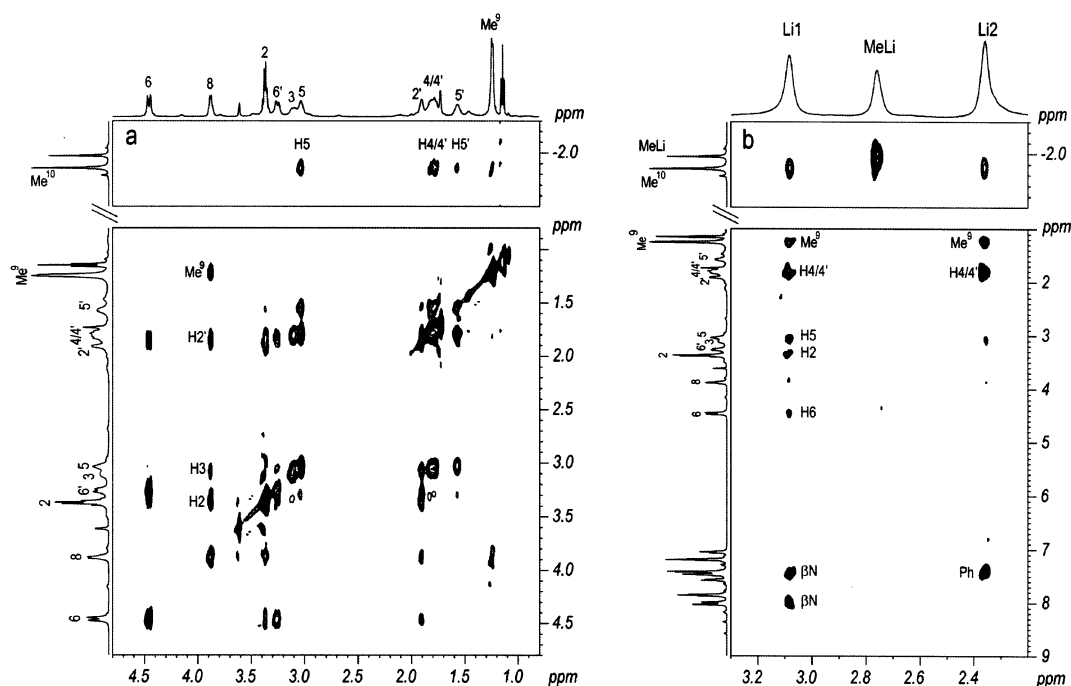


**Figure 5.** Mixed-aggregate  $[^6\text{Li}]\text{-3c}$  in  $\text{THF-}d_8$  solution at  $-78^\circ\text{C}$ . (a)  $^1\text{H}/^1\text{H}$  NOESY recorded with a mixing time ( $\tau_m$ ) of 600 ms. (b)  $^6\text{Li}/^1\text{H}$  HOESY recorded with a mixing time ( $\tau_m$ ) of 1 s.

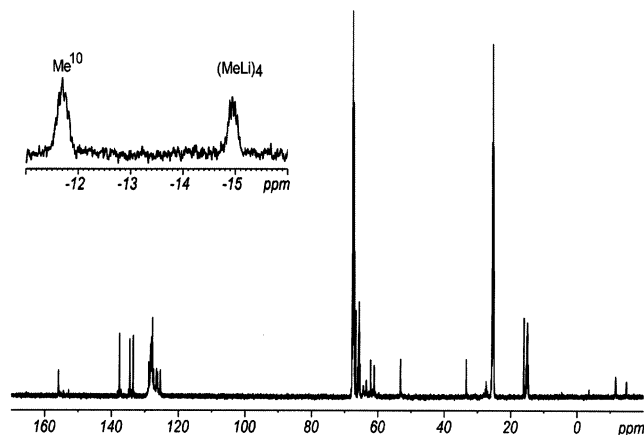


**Figure 6.** One-dimensional  $^{13}\text{C}$  spectrum of mixed-aggregate  $[^6\text{Li}]\text{-3c}$  in  $\text{THF-}d_8$  solution at  $-78^\circ\text{C}$ .

The most interesting signals on the  $^{13}\text{C}$  spectrum (Figure 6) are those at  $-11.70$  (quintet,  $J = 8.0$  Hz) and at  $-14.94$  ppm (heptet,  $J = 6.1$  Hz) that characterize the carbon of methyl-lithium in complex **3c** and free methyl-lithium, respectively. These multiplicities are in fine agreement with the presence of, respectively, two and three  $^6\text{Li}$  ( $I = 1$ ) nuclei around these carbons. Both chemical shifts and coupling constants are in good accord with reported values<sup>24</sup> and  $J$  roughly follows the empirical rule  $^1J(^{13}\text{C}, ^6\text{Li}) = 17/n$  (Hz),  $n$  being the number of  $^6\text{Li}$  nuclei bonded to the considered  $^{13}\text{C}$ .

The  $^6\text{Li}$  spectrum (Figure 7a) displays three singlets at 3.08, 2.76, and 2.36 ppm. Using the doubly labeled  $^{15}\text{N}, ^6\text{Li}$  complex **3c**, only the  $\text{Li}^1$  (as defined in Figure 2) signal became a doublet ( $J = 1.3$  Hz, Figure 7b), as expected from our folded model. Concomitantly, the  $^{15}\text{N}$  spectrum shows a broad singlet (for the reasons mentioned previously) at 53.9 ppm (Figure 7c). In quantitative integration conditions (relaxation delay  $d1 = 40$  s), the signals at 3.08 and 2.36 ppm proved to be in a 1:1 ratio.

The  $^6\text{Li}/^1\text{H}$  HOESY experiment (Figure 5b) displayed strong cross-couplings between the two lithium singlets at 3.08 and 2.36 ppm and the complexed  $\text{Me}^{10}$  proton singlet at  $-1.86$  ppm, whereas the 2.76-ppm lithium singlet correlated with that of free methyl-lithium proton singlet at  $-1.98$  ppm. The assignment of each lithium belonging to the complex was further confirmed by the HOESY experiment that showed cross-couplings between  $\text{Li}^1$  and  $\text{H}^6$  plus two protons of the  $\beta$ -naphthyl nucleus. These correlations were not observed for  $\text{Li}^2$ . Several other clues about the overall arrangement of the complex were also obtained from this heteronuclear experiment. Both lithium cations indeed correlate to methyl  $\text{Me}^9$  and  $4/4'$  proton(s). On the other hand, only  $\text{Li}^2$  interacts with some phenyl protons, whereas only  $\text{Li}^1$  correlates to  $\text{H}^5$  and  $\text{H}^2$  (in addition to  $\text{H}^6$  and the  $\beta$ -naphthyl protons mentioned above). All these observations are consistent with the arrangement of **3c** displayed in Figure 2. The orientation of the methyl-lithium along the concave ("endo", Figure 1b) face of the folded lithium amide could be confirmed by the  $^1\text{H}/^1\text{H}$  NOESY (Figure 5a), which displayed a meaningful correlation between  $\text{H}^8$  and  $\text{H}^2$  as well as the complexed  $\text{Me}^{10}$  and  $\text{H}^4/\text{H}^5$ . This arrangement, different from that observed for complex **3b**,<sup>8d</sup> imposes minimal conformational changes to the pyrrolidinic moiety when going from **2c** to **3c**. The complexation step most likely corresponds to a simple side-docking of the methyl-lithium along the  $\text{N-Li}$  bond. Thus, in the complex, the amide nitrogen returns to its tetrahedral environment. The alteration of complex **3c** topology with respect to that of **3b** is specially worth noting

- (21) (a) Gregory, K.; Schleyer, P. von R.; Snaith, R. *Adv. Inorg. Chem.* **1991**, 37, 47–151. For recent spectroscopical evidences see: (b) Grotjahn, D. B.; Sheridan, P. M.; Al Jihad, I.; Ziurys, L. M. *J. Am. Chem. Soc.* **2001**, 123, 5489–5494.
- (22) Fressigné, C.; Maddaluno, J.; Giessner-Pretre, C.; Silvi, B. *J. Org. Chem.* **2001**, 66, 6476–6479.
- (23) (a) Seitz, L. M.; Brown, T. L. *J. Am. Chem. Soc.* **1966**, 88, 2174–2178. (b) McKeever, L. D.; Waack, R.; Doran, M. A.; Baker, E. B. *J. Am. Chem. Soc.* **1969**, 91, 1057–1061. (c) Weiss, E.; Lamberts, T.; Schubert, B.; Cockroft, J. K.; Wiedenmann, A. *Chem. Ber.* **1990**, 123, 79–81.
- (24) Bauer, W.; Schleyer, P. v. R. *Adv. Carbanion Chem.* **1992**, 1, 89–175.

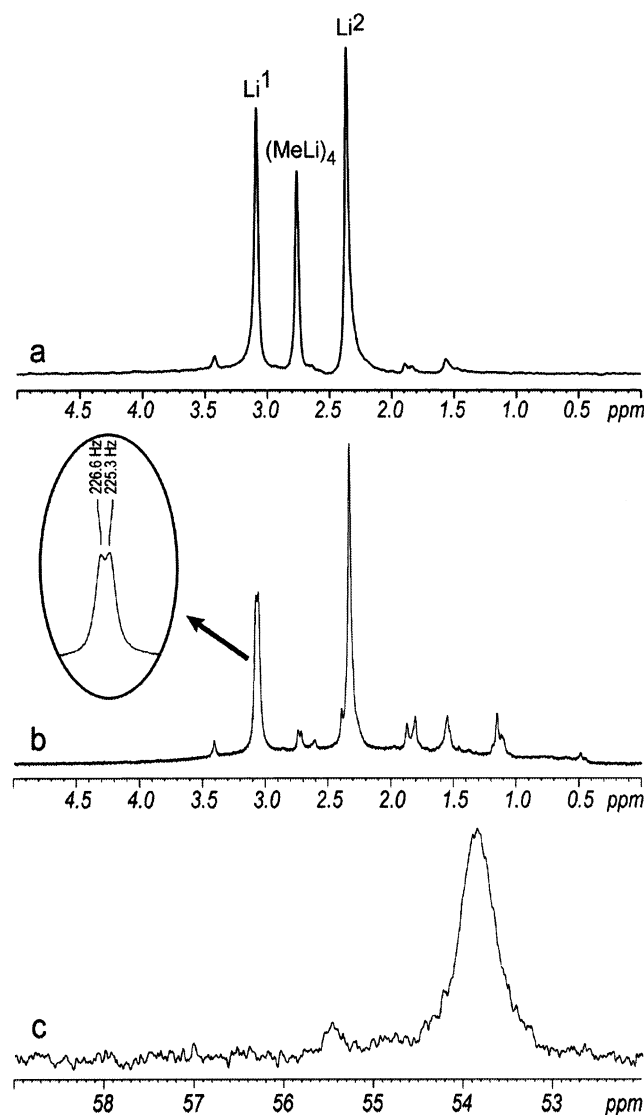


**Figure 7.** One-dimensional  $^6\text{Li}$  spectrum of mixed-aggregate  $[\text{Li}^6]-\mathbf{3c}$  in  $\text{THF}-d_8$  solution at  $-78^\circ\text{C}$ ; this sample contained an excess of  $\text{Me}^6\text{Li}$  at 2.76 ppm (a). One-dimensional  $^6\text{Li}$  spectrum of mixed-aggregate  $[\text{Li}^{15}\text{N}, \text{Li}^6]-\mathbf{3c}$  in  $\text{THF}-d_8$  solution at  $-78^\circ\text{C}$  (b). One-dimensional  $^{15}\text{N}$  spectrum of mixed-aggregate  $[\text{Li}^{15}\text{N}, \text{Li}^6]-\mathbf{3c}$  in  $\text{THF}-d_8$  solution at  $-78^\circ\text{C}$  (c).

in relation to the inversion of the sense of induction reported in Table 1 (entries 2 and 3). It provides further evidence for the central implication of these complexes in the control of the asymmetric induction. Other support to this hypothesis is provided by the results described below.

**(3*S*,8*R*)-*N*- $\beta$ -Naphthyl **2d/3d**.** The same investigation was performed with amine **1d**, a diastereomer of **1c** (Figure 2). The lithium amide **2d** was prepared as before, at  $-78^\circ\text{C}$  in  $\text{THF}-d_8$ , directly in the NMR tube according to the procedure used for **2c**. However, neither the  $^1\text{H}$  nor the  $^6\text{Li}$  spectra could aid interpretation of the structure of the compound in solution. The  $^1\text{H}$  spectrum (Figure 4S) exhibits large multiplets in the expected chemical shift regions, whereas the  $^6\text{Li}$  spectrum shows a large signal superimposed with more than 10 sharp peaks (Figure 5S). This indicates that lithium amide **2d** leads to a complex mixture of aggregates in solution, a phenomenon already encountered with amide **2a**.<sup>8d</sup> In this latter case, it had been assumed that the relatively small benzyl group was favoring an intermolecular

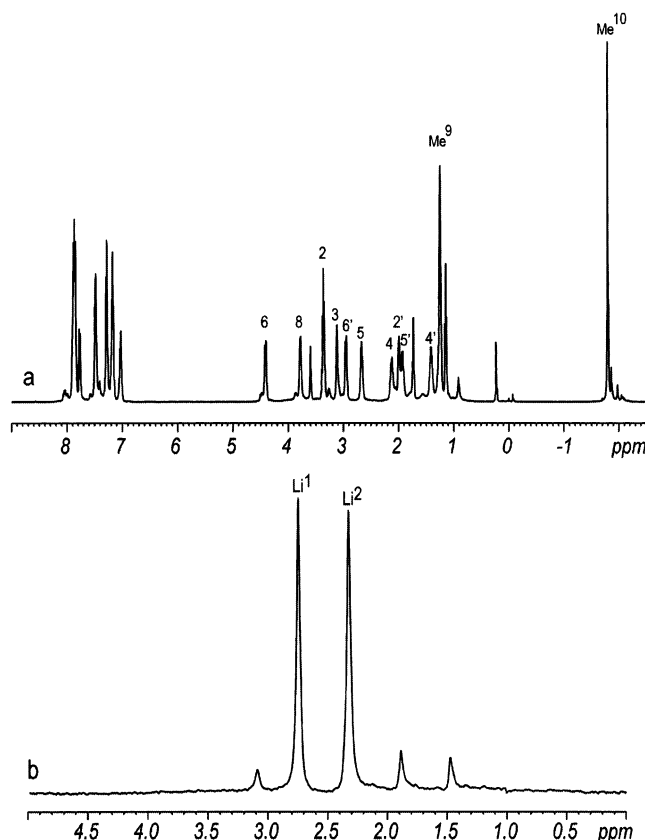


**Figure 8.** One-dimensional  $^1\text{H}$  (a) and  $^6\text{Li}$  (b) spectra of mixed-aggregate  $[\text{Li}^6]-\mathbf{3d}$  in  $\text{THF}-d_8$  solution at  $-78^\circ\text{C}$ .

aggregation over an intramolecular chelation of the lithium cation. By contrast, the more bulky benzhydryl appendage in **2b** was triggering the chelation rather than the aggregation. On steric grounds, the  $\alpha$ -methylbenzyl chain in **2c,d** can be considered as intermediate between the benzyl and benzhydryl ones. This threshold situation can explain that the (*S,S*) diastereomer behaves as the “bulky” amide and the (*S,R*) isomer adopts the “small” amide preferences. However, detailed structural investigations were restricted to **3d**, the compound of major interest.

The NMR spectroscopy study has been pursued with complex **3d**, and the one-dimensional  $^1\text{H}$  and  $^6\text{Li}$  NMR spectra obtained at  $-78^\circ\text{C}$  are featured in Figure 8. The resolution improves to an analytical level for both nuclei. The assignment of the proton signals was achieved by  $^1\text{H}/^1\text{H}$  COSY and  $^1\text{H}/^{13}\text{C}$  HMQC sequences (Figures 6S and 7S) and shows, for H<sup>2</sup>, H<sup>5</sup>, and H<sup>6</sup> splittings similar to those observed with **3c**. A singlet at  $-1.80$  ppm, representative of the complexed  $\text{Me}^{10}$ , is also observed, beside three small unidentified peaks at higher fields, one of those probably corresponding to a slight excess of free methyllithium.

Similarly to **3c**, the  $^{13}\text{C}$  spectrum (Figure 8S) displays a well-defined quintet ( $J = 8.4$  Hz, Figure 9a) at  $-11.83$  ppm, characteristic of the aggregated methyllithium. Both the multiplicity and the  $J$  value are in agreement with a 1:1 complex analogous to the previous ones. The  $^6\text{Li}$  spectrum (Figure 8b) exhibits two major singlets at 2.74 and 2.32 ppm, together with three minor peaks (further discussed in the case of **3f**). The two main peaks belong to a same structure as demonstrated by a  $^6\text{Li}/^6\text{Li}$  COSY spectrum (Figure 9b).



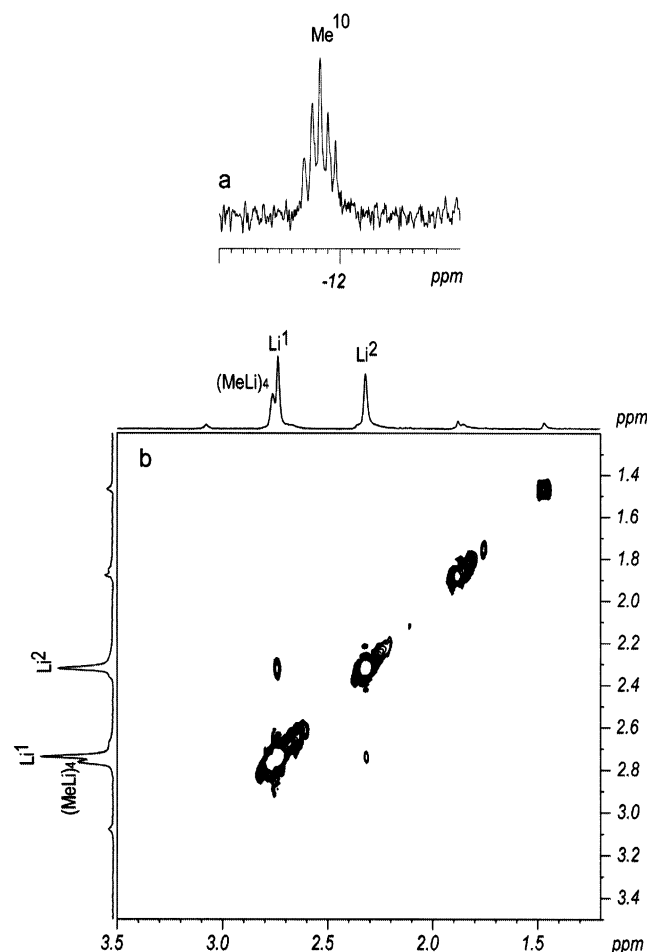


**Figure 9.** Blow-up of the one-dimensional  $^{13}\text{C}$  spectrum of mixed-aggregate  $[\text{Li}^6]\text{-3d}$  in  $\text{THF-}d_8$  solution at  $-78^\circ\text{C}$  (a). Two-dimensional  $^6\text{Li}/^6\text{Li}$  COSY contour plot spectrum ( $\tau = 250$  ms) of mixed-aggregate  $[\text{Li}^6]\text{-3d}$  in  $\text{THF-}d_8$  solution at  $-78^\circ\text{C}$  (b).

Both could be assigned through a  $^6\text{Li}/^1\text{H}$  HOESY experiment (Figure 10b, recorded on a sample containing a slight excess of methyllithium) that exhibits a cross-coupling between the low-field  $\text{Li}^1$  and  $\text{H}^6$  (but not between  $\text{Li}^2$  and these same protons). Significantly different from the case of **3c** is the appearance of correlations between  $\text{Li}^2$  and  $\text{H}^2/\text{H}^{2'}$  and the disappearance of the  $\text{Li}^2/\text{H}^4$  interactions mentioned for **3c**. The correlations observed between the two lithium nuclei and both  $\text{H}^2$  are probably due to a direct HOE effect (the  $\text{Li}^{1,2}\text{--H}^{2,2'}$  distances being, from theoretical results presented below, always inferior to  $4.2\text{ \AA}$ , that is fully compatible with such an effect). These observations strongly suggest that the conformation of complex **3d** resembles more that of **3b** than that of **3c**; that is to say that the methyllithium is lying along the “exo” face of the norbornyl moiety, as shown in Figure 2. The  $^1\text{H}/^1\text{H}$  NOESY experiment (Figure 10a) supports this assumption through the  $\text{Me}^{10}\text{--H}^2$  as well as  $\text{H}^8\text{--H}^4$  and (weaker)  $\text{H}^8\text{--H}^5$  correlations. These latter data also provide information on the position of the chiral appendage within the complex which seems to orientate as depicted in Figure 2.

Therefore, it seems that the configuration of the lateral chiral center controls the overall topology of the amide-methyllithium complex, and seems responsible for the inversion of the sense of the observed asymmetric induction in the enantioselective alkylation of *o*-toluadehyde (Table 1, entries 3 and 4). Molecular

models show that this alteration in the mode of complexation is probably due to steric effects. In both the “endo” (such as **3c**) and “exo” (such as **3b** or **3d**) type of complexes, the phenyl group on  $\text{C}^8$  is always on the “outer” portion of space. The steric strains can then be minimized by orienting the  $\text{H}^8$  proton toward the more crowded region. This actually defines the preference for the “exo” or “endo” arrangement. In the endo complex **3c**,  $\text{H}^8$  faces the  $\text{C}^2$  bridge, whereas in the exo complex **3d**, this same proton is oriented toward the norbornyl concave face.

**(3*S*,8*S*)-*N*-Methyl 2e/3e.** NMR spectra of lithium amide **2e** from amine **1e** (Scheme 2) in  $\text{THF-}d_8$  at  $-93^\circ\text{C}$  afforded the sharpest line shapes. The complex  $^1\text{H}$  and  $^6\text{Li}$  spectra (Figures 9S and 10S) suggest that we are dealing with a mixture of aggregated amide similar to that encountered in amide **2d**. Interestingly, **2c** gives rise to a simple entity in solution. Thus, and by contrast with the previous complexes, the structure of the amides does not seem to be controlled only by the lateral chiral chain but also by the exact nature of the pyrrolidinic nitrogen substituent. It is reasonable to assume that the smaller methyl appendage on this nitrogen in **2e** decreases its steric hindrance and can promote aggregation phenomena that are less likely with the bulky  $\beta$ -naphthyl group borne by **2c**. Once again, detailed structural investigations were restricted to **3e**.

The  $^1\text{H}$  NMR spectrum of **3e** (Figure 11S) shows the presence of a slight excess (0.23 equiv) of methyllithium. All signals could be assigned from the spectroscopic methods described above. The  $\text{H}^2$  and  $\text{H}^5$  signals split also as described for **2c/3c**, whereas  $\text{H}^4$  and  $\text{H}^{4'}$  merge at 1.75 ppm. Differing from previous cases, a series of small peaks corresponding to those of amide **2e** remains despite the excess of methyllithium. This observation is confirmed by the  $^6\text{Li}$  spectrum (Figure 11a) that exhibits two peaks (at 2.61 and 2.21 ppm) assigned to the 1:1 complex **3e** (Figure 2), together with the free methyllithium singlet (2.71 ppm) superimposed over a profile of smaller signals similar to that of amide **2e**. Unexpectedly, the addition of one more equivalent of methyllithium did not change the relative ratio **3e/2e**, even when the temperature was raised to  $20^\circ\text{C}$ . This observation prompted us to add 2 equiv of methyllithium directly to the amine **1e** in an attempt to obtain complex **3e** without stopping at the amide **2e**. In this case, the  $^6\text{Li}$  spectrum (Figure 11b) indicates that this approach is reasonable because only **3e** and free methyllithium signals are visible.

The topology of the complex thus obtained could then be established from the  $^6\text{Li}/^1\text{H}$  HOESY (Figure 12S) and  $^1\text{H}/^1\text{H}$  NOESY (Figure 13S) spectra that indicate a  $\text{Li}^2/\text{H}^4$ ,  $\text{H}^5$  proximity on one hand, and  $\text{Li}^2/\text{Me}^{10}$  on the other. The  $\text{H}^2/\text{H}^8$  NOESY cross-peak confirms that the methyllithium is oriented toward the endo face of the amide, as in complex **3c** (Figure 2). Therefore, this type of arrangement seems to be associated with the (*S,S*) configuration of the 3-AP-derived amides **2c,e**.

**(3*S*,8*R*)-*N*-Methyl 2f/3f.** Once again, a first equivalent of methyllithium was added, at  $-78^\circ\text{C}$ , to a  $\approx 0.2\text{ M}$  amine **1f** (Scheme 2) solution in  $\text{THF-}d_8$ , and the spectra recorded at  $-93^\circ\text{C}$ . The simple  $^1\text{H}$  spectrum obtained (Figure 14S) presents the expected signals with splittings similar to those described above for the bridged species. The  $^6\text{Li}$  spectrum (Figure 15S) is also simple but displays two sharp peaks (1:1) at 1.67 and 1.33 ppm, whereas the  $^1\text{H}$  spectrum shows no methyllithium (free or complexed). Therefore, a dimeric structure **11** (Figure 14),

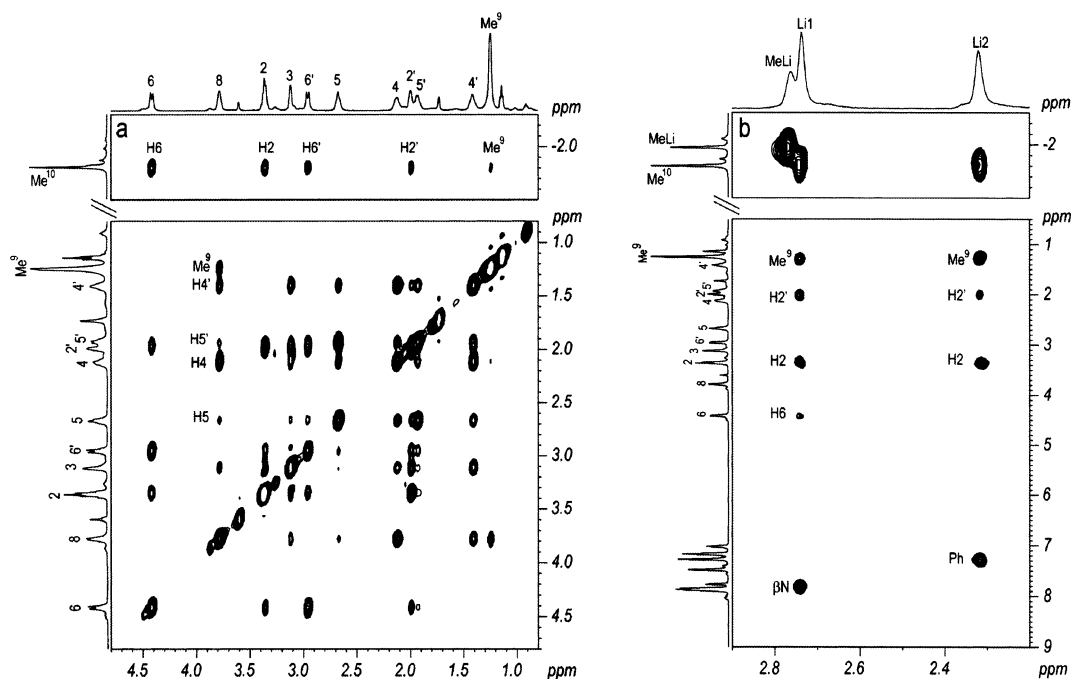


**Figure 10.** Mixed-aggregate  $[\text{Li}^6]\text{-3d}$  in  $\text{THF-}d_8$  solution at  $-78^\circ\text{C}$ : (a)  $^1\text{H}/^1\text{H}$  NOESY recorded with a mixing time ( $\tau_m$ ) of 600 ms. (b)  $^6\text{Li}/^1\text{H}$  HOESY recorded with a mixing time ( $\tau_m$ ) of 1 s.

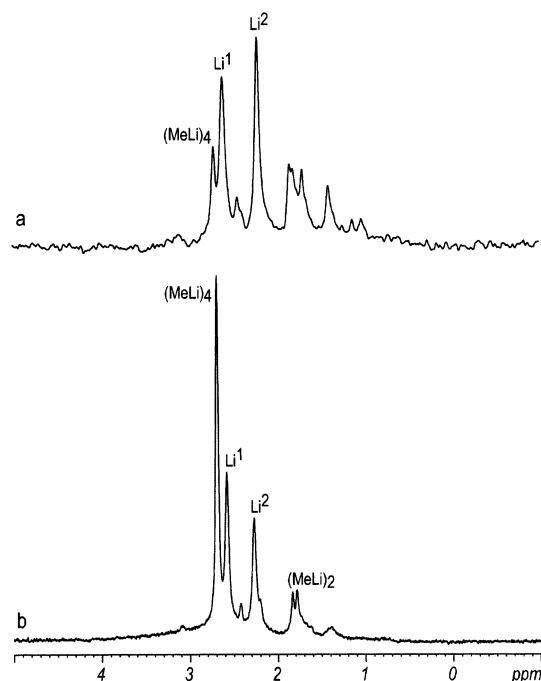


**Figure 11.** One-dimensional  $^6\text{Li}$  spectrum of lithium amide  $[\text{Li}^6]\text{-3e}$  in  $\text{THF-}d_8$  solution at  $-93^\circ\text{C}$ : (a) as obtained by two successive additions of 1 equiv of  $\text{Me}^6\text{Li}$  on amine **1e**; (b) as obtained by the direct addition of 2 equiv of  $\text{Me}^6\text{Li}$  on amine **1e**.

symmetrical but incorporating two different lithium cations for **2f** seems to be formed. Spectroscopic studies to determine its structure have remained unsuccessful so far.

The addition of 1 equiv of  $[\text{Li}^6]\text{-MeLi}$  to the NMR tube leaves the above-mentioned amide structure intact, a behavior reminiscent of the incomplete mixed-aggregation of the (*S,S*) diastereomer **2e**. The  $^1\text{H}$  spectrum (Figure 16S) displays the huge singlet of free tetrameric methyllithium ( $-2.06$  ppm),

together with a set of tiny peaks corresponding to dimeric methyllithium and to the mixed aggregate (vide infra). This hypothesis is supported by the  $^6\text{Li}$  spectrum (Figure 12b) that exhibits the two singlets of the lithium amide (at 1.67 and 1.33 ppm) together with those of the “free” methyllithium (at 2.71 and 1.85 ppm, for the tetramer and dimer, respectively, as checked on a THF solution of pure methyllithium depicted in Figure 12a). Two small peaks (at 2.44 and 2.19 ppm) of the mixed complex can also be seen in Figure 12b. Raising the temperature to  $-13^\circ\text{C}$  for 15 min and cooling back to  $-93^\circ\text{C}$  does not increase the reactivity of the amide. The experimental protocol followed to prepare these NMR samples is identical to that applied in the asymmetric alkylation of *o*-tolualdehyde.<sup>25</sup> Therefore, the lower chemical yields associated with the use of amides **2e,f** (Table 1, entries 5 and 6) could be related to the formation of a comparable dimeric amide that would not aggregate with butyllithium, but would react directly with the aldehyde to provide an  $\alpha$ -amino alcoholate of which formation has been evidenced in comparable cases.<sup>8c,12</sup>

We next tried to add directly 2.3 equiv of methyllithium onto the amine **1f**. This resulted in the formation of complex **3f** (Figure 2), as indicated by both the  $^1\text{H}$  and  $^6\text{Li}$  spectra (Figures 17S and 12c). The latter exhibits five main peaks, corresponding to some excess “free” methyllithium (2.71 ppm), the two peaks of the 1:1 usual complex (2.44 and 2.19 ppm), and those of the starting amide dimer (1.67 and 1.33 ppm). Thus, despite the excess of methyllithium about 30% of dimeric amide persists. A complementary  $^6\text{Li}/^6\text{Li}$  exchange spectroscopy (EXSY) experiment was performed on the same sample to get information on the exchanges taking place between these different lithium cations. This spectrum (Figure 13) shows that the lithium

(25) This is worth underlining with respect to the relatively low chemical yields reported in entry 6 of Table 1. The complex **3f** used in the experiments is indeed prepared by addition of 1.1 equiv of alkylolithium at  $-20^\circ\text{C}$  during 20 min then 1.5 equiv  $\text{MeLi}$  at the same temperature before cooling down to  $-78^\circ\text{C}$ . This protocol is therefore likely to provide a medium containing relatively large amounts of uncomplexed lithium amide **2f**.

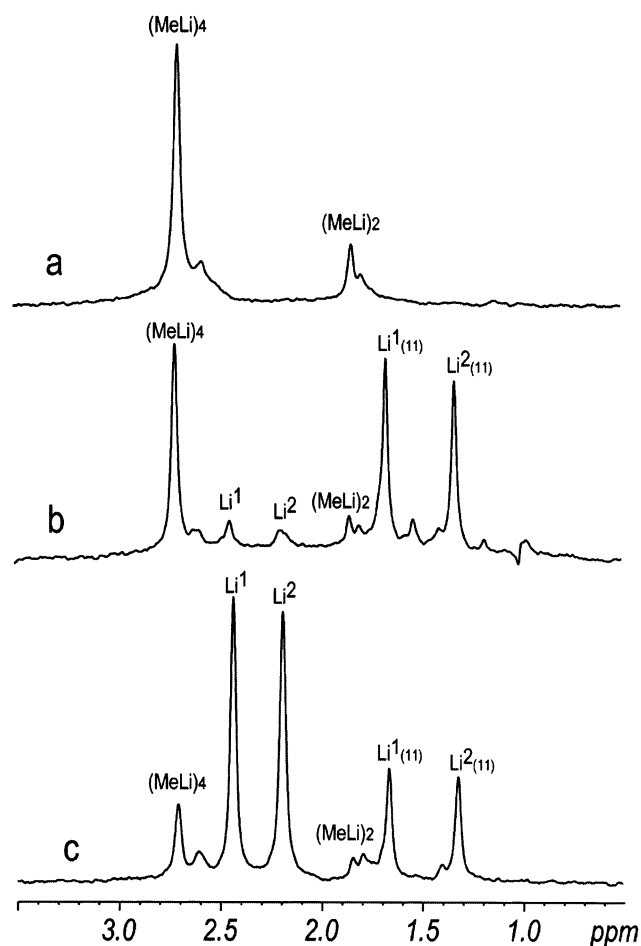


**Figure 12.** One-dimensional  $^6\text{Li}$  spectrum of (a) pure methylolithium, (b) a mixture of methylolithium and dimer **11** of lithium amide  $[\text{}^6\text{Li}]\text{-2f}$ , and (c) a mixture of methylolithium, dimer **11** of lithium amide  $[\text{}^6\text{Li}]\text{-2f}$ , and mixed-aggregate  $[\text{}^6\text{Li}]\text{-3f}$ .

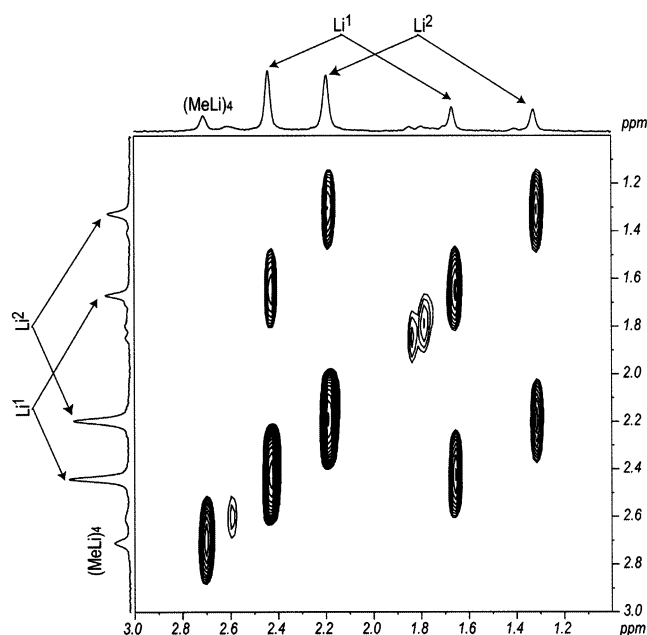


**Figure 13.** Two-dimensional  $^6\text{Li}/^6\text{Li}$  EXSY contour plot spectrum of mixed-aggregate  $[\text{}^6\text{Li}]\text{-3f}$  in  $\text{THF-}d_8$  solution at  $-93\text{ }^\circ\text{C}$ .

nuclei belonging to a same complex exchange slowly with respect to the exchange taking place between those of the mixed

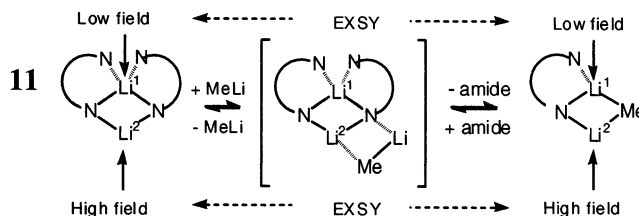


**Figure 14.** Proposed equilibria between monomeric and dimer **11** of lithium amide **2f** and mixed-aggregate **3f**.

aggregate and those of the dimeric amide, as indicated by a strong cross-coupling between the low-field lithiums. The same remark applies to the high-field lithiums. The methylolithium does not couple with any other signal.

These data suggest an additive mechanism<sup>26</sup> proceeding through a set of equilibria such as those depicted in Figure 14, which underline the similarities between the lithium environments when going from the dimeric amide **11** to the mixed aggregate.

The  $^1\text{H}$  recording (Figure 17S) shows a well resolved spectrum exhibiting a large peak for the complexed methylolithium at  $-2.17$  ppm, whereas the smaller signal at  $-2.05$  ppm corresponds to the 0.3 equiv of excess MeLi in the tube. These assignments were made through the same  $^1\text{H}/^1\text{H}$  COSY and  $^1\text{H}/^{13}\text{C}$  HMQC (not shown), as well as  $^1\text{H}/^1\text{H}$  NOESY (Figure 18S) and  $^6\text{Li}/^1\text{H}$  HOESY (19S) set of experiments. The most striking features in these data are the  $\text{H}^8/\text{H}^4$  and  $\text{Me}^{10}/\text{H}^2$  cross-peak correlations, as well as those between  $\text{Li}^2$  and  $\text{H}^2$ . These correlations suggest that the methylolithium is oriented toward the exo face of the norbornyl arrangement, whereas the amino chiral appendage lies along the endo face (Figure 2) and adopts a conformation similar to that observed above for **3d**. The similarity between these arrangements is once more remarkable because it indicates that the (*S,R*) diastomeric amides **2d** and **2f** both prefer the “exo” mode of complexation.

The differences stemming from the ways the mixed aggregate **3f** is prepared (addition of sequentially one then another, or directly 2 equiv, of methylolithium onto the amine **1f**) suggest that the energy barrier between an eventual amide **2f** dimer **11** evoked above and **3f** is sufficiently high to prevent the conversion of the former into the latter, even in the presence of an excess of methylolithium. They also indicate that the kinetics favor the mixed-aggregation over the dimerization because the synthesis of the lithium amide **2f** in the presence of an excess of methylolithium leads directly to **3f**, almost avoiding the irreversible formation of **11**.

**Theoretical Studies.** The experimental conditions for the NMR recordings, from which the geometrical arrangements were deduced, have at least two important consequences: (1) The low temperature ( $-78\text{ }^\circ\text{C}$ ) of the medium is compatible with both a kinetically or thermodynamically controlled complexation. (2) The solvent used, THF, is known to be associated with large interaction energies ( $10\text{--}20\text{ kcal/mol}$ )<sup>13,14c,27</sup> with organolithium compounds. Therefore, the solvent might determine the aggregation of the complexes under study.

We thus thought that a theoretical investigation on these systems could provide an indication on the leading factor underlying the conformational preferences. The similarity

(26) We thank one of the referees for suggesting this mechanism.

(27) Tacke, M. *Eur. J. Inorg. Chem.* **1998**, 537–541.

**Table 2.** DFT (B3P86) and MP2 Energy Values (in a.u.) Calculated with the 6-311++G\*\* Basis Set for the DFT-Optimized “Exo” and “Endo” Arrangements of the Gas Phase **3e** and **3f** Complexes<sup>a</sup>

	B3P86		MP2//B3P86	
	“endo”	“exo”	“endo”	“exo”
<b>3e</b>	−673.7839(0.2)	−673.7842(0.0)	−669.3876(0.6)	−669.3885(0.0)
<b>3f</b>	−673.7835(0.0)	−673.7830(0.3)	−669.3873(0.0)	−669.3871(0.1)

<sup>a</sup> Relative stabilities (in kcal/mol) are in parentheses.

between the experimental results (on both induction and conformational grounds) given by the *N*-CH<sub>2</sub>- $\beta$ -naphthylpyrrolidines **2c,d** and the *N*-methylpyrrolidines **2e,f**, altogether with the 17 additional atoms in the former compounds, prompted us to limit the calculations to the latter molecules.

The computational procedures we have followed are detailed in the Supporting Information. The theoretical results presented here do not include data on the amides **2e,f**, which are not the main object of this study. We have considered directly the complexes **3e,f**. Because previous results on the unsubstituted 3-AP have shown the exo and endo conformers to be isoenergetic,<sup>13</sup> we undertook on **3e** diastereomer an investigation of the influence of the basis set and functional used for the computations on the energy difference between the two arrangements. The results, reported in Table 1S, show that this difference is only marginally sensitive to the basis set extension or functional used.

The first optimizations have dealt with the isolated species in the gas phase. The results obtained with the 6-311++G\*\* basis set and the B3P86 hybrid functional, for both the endo and exo arrangements of **3e** and **3f**, are gathered in Table 2. This functional was chosen for the sake of consistency with previous studies.<sup>10a,13</sup> Despite the size of the basis set, only very small numerical differences are found between the two conformations of both complexes. To determine the sensitivity of the calculated energy differences to the computational procedure, we ran single point calculations using second-order Moller-Plesset theory (MP2) on the B3P86-optimized geometries. The size of the basis set precluding MP2 full optimizations. The corresponding results, reported in Table 2, show that if the total energy absolute values differ by more than 4 a.u., the energy differences are quite similar to those given by DFT, that is inferior to 1 kcal/mol. The only minor difference concerns the method/conformation relationship: the DFT seems to be more in favor of the endo conformers than MP2 and vice versa. This set of results should be, under thermodynamics control, associated to the coexistence of the endo and exo arrangements in solution, in discrepancy with the above NMR data. This and the very small calculated energy gap prompted us to consider possible solvation effects.

We resorted to a discrete solvation model incorporating three molecules of dimethyl ether (two on Li<sup>1</sup> and one on Li<sup>2</sup>, Figure 15), which put each lithium cation in a “standard” tetrahedral coordination sphere.<sup>14a,28</sup> For these calculations, a shift from the 6-311++G\*\* to the 6-311+G\*\* basis set was used because of near-linear dependence problems. The optimized arrange-

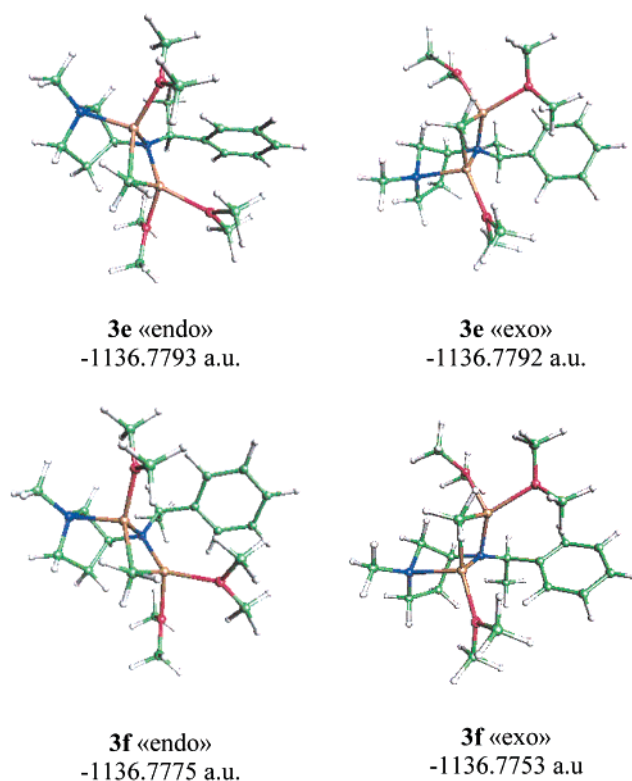


**Figure 15.** Quantum chemical optimized geometrical arrangements of the “endo” and “exo” conformations of the mixed aggregates **3e** and **3f**.

ments depicted in Figure 15 show, for the core of the complex, a striking similarity with the gas-phase results. In particular, the norbornyl-like topology is preserved, in agreement with the corresponding NMR data. Similarly, the energy differences found between the exo and endo situations (as reported in Figure 15) remain relatively negligible. We find indeed that the “endo” conformations of the (*S,S*) and (*S,R*) diastereomers **3e** and **3f** are favored by 0.1 and 1.4 kcal/mol, respectively. These values tend to show that the first solvation shell has only a minor influence on the aggregation pattern of these systems.

The difference between the NMR results, which seems to indicate one favored type of complex for each lithium amide diastereomer,<sup>29</sup> and the theoretical data, which do not find any significant preference for one or the other arrangement for both diastereomers, tend to confirm a purely kinetic control of the mixed aggregation phenomenon. Indeed, the species that are formed first are not necessarily the most stable. If this is the case, the calculation of the lithium nuclear magnetic shielding constants ( $\sigma$ ) might support the kinetic control hypothesis provided that the variation of the calculated chemical shift difference between the two lithiums when going from **3e** to **3f** is in qualitative agreement with the measured one. Our previous results concerning lithium shieldings in the mixed aggregate between methyllithium and 3-methylamino-*N*-methylpyrrolidine suggested that these data could be of reasonable accuracy despite the relatively narrow chemical shift range of <sup>6</sup>Li.<sup>13</sup> Bearing in mind that the calculated  $\sigma$  values decrease when the experimental  $\delta$  values increase (both expressed in parts per million),

(28) See inter alia: (a) Kallman, N.; Collum, D. B. *J. Am. Chem. Soc.* **1987**, *109*, 7466–7472. (b) Clegg, W.; Edwards, A. J.; Mair, F. S.; Nolan, P. M. *Chem. Commun.* **1998**, 2324. (c) van Vliet, G. L. J.; de Kanter, F. J. J.; Schakel, M.; Klumpp, G. W.; Spek, A. L.; Lutz, M. *Chem. Eur. J.* **1999**, *5*, 1091–1094. (d) Pye, C. C. *Int. J. Quantum Chem.* **2000**, *76*, 62–76.

(29) Warming the sample up to room temperature does not equilibrate the endo or exo complexes into a mixture. This suggests that the complex obtained is both kinetically and thermodynamically favored or that the interconversion barrier between these two forms is too high to be overcome before THF begins to react with these strong bases.



**Table 3.** B3P86 Energy Values Calculated with the 6-311+G\*\* Basis Set,  $^6\text{Li}$  Nuclear Magnetic Shielding Constants for the “Exo” and “Endo” Arrangements of the Solvated **3e** and **3f** Complexes, and Corresponding  $\Delta\delta$  Experimental Values (in parts per million)

complex	$E^a$	$\sigma(\text{Li}^1)$	$\sigma(\text{Li}^2)$	$\Delta\sigma$	$\Delta\delta$
<b>3e</b> “endo”	−1136.7793 (0.0)	88.85	90.27	1.42	0.45
<b>3e</b> “exo”	−1136.7792 (0.1)	89.28	89.88	0.60	
<b>3f</b> “endo”	−1136.7775 (0.0)	89.32	90.35	1.03	0.25
<b>3f</b> “exo”	−1136.7753 (1.4)	89.48	90.35	0.87	

<sup>a</sup> Energy values as in Table 2.

the data reported for the solvated complexes in Table 3 show that; (i)  $\text{Li}^1$  is in all cases less shielded than  $\text{Li}^2$  in agreement with experimental observations; (ii) the calculated chemical shift difference between  $\text{Li}^1$  and  $\text{Li}^2$  is significantly larger than the corresponding measured values. The calculated values show also that the chemical shift difference between the two lithium nuclei ( $\Delta\delta$ ) is larger for the endo than for the exo conformations. The larger experimental data obtained for **3e** with respect to **3f** suggest that **3e** could adopt an endo arrangement and **3f** an exo one. These results tend to further support the hypothesis of a kinetic control, altogether with the large interaction energy value between the lithium amide and the methyllithium in the aggregates ( $>49$  kcal/mol in the gas phase in all cases). Such large figures leave little chance for a reversible process. The theoretical validation of this hypothesis, however, would require *ab initio* molecular dynamics (Car-Parrinello) studies that lie beyond the capabilities of the static quantum chemistry methods used for the present study.

## Conclusion

Experimental multinuclear NMR results and DFT calculations show that the pyrrolidine ring of *N*-substituted 3-aminopyrrolidines lithium amides tends to adopt a norbornyl-like folding. On these structures, the NMR data indicate that methyllithium binds along the “concave” (endo) face in the cases of the (3*S*,8*S*) diastereomers **2c,e** or along the “convex” (exo) one in that of (3*S*,8*R*) diastereomers **2d,f**. This result implies that the topology of the complexes formed between alkylolithiums and 3-AP lithium amides is completely determined by the relative configuration of the lateral asymmetric center with respect to that on the pyrrolidine ring. Therefore, both types of complexes can be obtained on a simple swap of the absolute configuration of the lateral (commercial) amine. The DFT theoretical calculations on these complexes, solvated by three molecules of dimethyl ether, indicate that there is no significant thermodynamical preference for one or the other arrangement. If dimethyl ether is an appropriate model for THF, this result suggests that the methyllithium binding occurs under a purely kinetic control.

The two alkylolithium binding modes thus correspond to the two different absolute configurations of the lateral nitrogen atom which becomes chiral upon complexation. Although the “endo” mode of binding (as observed with the complexes **3c,e**) corresponds to a (3*S*,7*R*,8*S*) situation, the “exo” aggregation stereochemistry (associated to complexes **3d,f**) can be described as (3*S*,7*S*,8*R*). This observation is of special interest because it suggests that a 3-AP lithium amide with a racemic carbon 3 and a chiral carbon 8 (for instance *S*) would provide *ee* comparable with those obtained with pure (3*R*,8*S*) or pure (3*S*,8*S*) 3-AP, the two diastereomers leading to the formation of aggregates presenting “opposite” conformations but responsible for the same sense of induction (Figure 16).

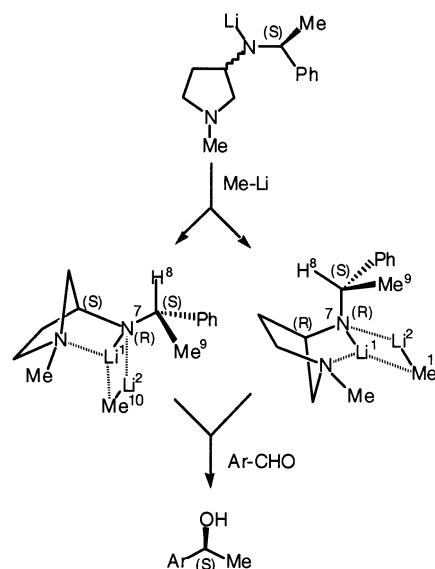


**Figure 16.** Proposed conformations for  $\text{Me}^6\text{Li}$  mixed aggregates with a mixture of (3*S*,8*S*) and (3*R*,8*S*) 3-AP lithium amide, leading to (*S*)-1-phenylethanol.

Because the change in the methyllithium/3-AP lithium amide-binding mode parallels an almost total induction reversal in the asymmetric alkylation model reaction (Table 1), it is tempting to associate one complex with one sense of induction. The Curtin–Hammett principle, which only applies if the system is under thermodynamic control, forbids such a reasoning, because minor unobserved complexes can be responsible for the effective chemical pathway. Therefore, a detailed study of the aromatic aldehyde docking on type-3 complexes followed by the determination of the condensation transition state remains to be done to get insight into the factors responsible for the enantioselectivity of this reaction.

Finally, we think this work helps to open a little the “black-box” surrounding the asymmetric version of one of the fundamental reactions of organic chemistry. It shows that the in-depth study of the chiral entity involved in an enantioselective reaction can provide essential information regarding the exact mechanism of asymmetry transfer. Last but not least, these results also suggest alterations that can be brought to the partners of the reaction to modulate and improve the enantiomeric excesses. The corresponding experiments and computations are currently under way.

**Acknowledgment.** The 500 MHz NMR spectrometer used in this study was supported by grants of the Conseil Régional de Haute-Normandie (France). A.C. is grateful to the inter-regional RINCOF program for a postdoctoral grant. We also thank the Centre de Ressources Informatiques de Haute-Normandie (CRIHAN, Mont Saint Aignan) within the framework of the “Bassin Parisien Régional Plan” (CPIBP) local modeling center for engineering sciences contract (article 12) and of the “Réseau Normand pour la Modélisation Moléculaire”, as well as the Centre de Calculs pour la Recherche (CCR, Université P. & M. Curie, Paris) and the Institut du Développement et des Ressources en Informatique Scientifique (IDRIS, Orsay) for computer time. We also warmly thank Prof. Kym F. Faull (UCLA) for proof-reading this manuscript.

**Supporting Information Available:** Experimental details and characterization data, computational procedures, spectra for **2c–f** and **3c–f**, and table listing calculated energy values for the **3e**

complex (PDF). This material is available free of charge via the Internet at <http://pubs.acs.org>.

JA016945D